

Determination of pore-size distribution in low-dielectric thin films

D. W. Gidley^a and W. E. Frieze

Department of Physics, University of Michigan, Ann Arbor, Michigan 48109

T. L. Dull, J. Sun, and A. F. Yee

Department of Materials Science and Engineering, University of Michigan, Ann Arbor, Michigan 48109

C. V. Nguyen

IBM Almaden Research Center, San Jose, California 95120

D. Y. Yoon

Department of Chemistry, Seoul National University, Seoul 151-742, Korea

(Received 5 August 1999; accepted for publication 14 January 2000)

Positronium annihilation lifetime spectroscopy is used to determine the pore-size distribution in low-dielectric thin films of mesoporous methylsilsequioxane. A physical model of positronium trapping and annihilating in isolated pores is presented. The systematic dependence of the deduced pore-size distribution on pore shape/dimensionality and sample temperature is predicted using a simple quantum mechanical calculation of positronium annihilation in a rectangular pore. A comparison with an electron microscope image is presented. © 2000 American Institute of Physics. [S0003-6951(00)03810-9]

There is currently a great deal of interest in introducing and characterizing nanometer-sized voids into thin silica and polymer films. Such porous films are being intensely pursued by the microelectronics industry as a strategy for reducing the dielectric constant of interlayer insulators in microelectronic devices. Unfortunately, there are relatively few techniques capable of probing the average pore size and/or the pore size distribution in submicron films on thick substrates. This is particularly true if the voids are closed (not interconnected) so that gas absorption techniques are not available. Neutron scattering¹ and positronium annihilation lifetime spectroscopy (PALS)² have recently been used to determine an average pore size in silica films and Doppler broadening positron spectroscopy³ has been used to probe open volume in silsesquioxane films. None of the methods can determine a pore-size distribution in porous silica (this is apparently a fundamental limitation in neutron scattering, whereas with PALS the limitation is a result of the complete interconnectedness of the silica pores²). In closed-pore systems PALS may be uniquely capable of deducing a pore-size distribution, even in films buried under metal overlayers. The goal of this letter is to develop this PALS capability in a porous film that nominally has closed pores.

The sample films studied were formed by spin casting a homogeneous mixture of poly(methylsilsequioxane) (MSSQ) and 10% by weight poly(caprolactone) (PCL), a degradable porogen. Upon heating to 250 °C the MSSQ prepolymer polymerizes and crosslinks, causing the PCL phase to separate into domains. At 430 °C the PCL has degraded and volatilized, leaving behind a mesoporous, 0.8- μm -thick MSSQ film⁴ with a dielectric constant of 2.5. We have performed a detailed PALS study of this system for varying PCL weight fractions, sample temperature, and processing conditions. Our focus here is to develop a physical model of

the diffusion, trapping, and annihilation of positronium (Ps) in these films in order to determine the pore-size distribution from the PALS spectrum.

In using PALS with thin films^{5,6} a focused beam of several keV positrons forms positronium (Ps, the electron-positron bound state) over a distribution of depths that depends on the beam energy. Ps inherently localizes in the pores where its natural lifetime of 142 ns is reduced by annihilation with molecular electrons during collisions with the pore surfaces. The collisionally reduced lifetime is correlated with void size.² This correlation is the key feature that permits a PALS lifetime distribution to be transformed into a pore-size distribution if Ps is trapped in isolated voids of varying sizes. This was not the case in the interconnected voids of porous silica films² where the highly mobile Ps atoms all sample the same average pore size and hence annihilate with a single, average lifetime. Porous MSSQ presents a distribution of Ps lifetimes.

Lifetime spectra acquired before and after decomposition of the PCL are compared in Fig. 1. Data are typically acquired with an 8000 channel time-to-digital converter over a time range of 1.25 μs . Initially we used the standard program POSFIT to fit discrete lifetimes to this spectrum. Prior to PCL decomposition the “unfoamed” film presents lifetimes consistent with those in bulk MSSQ (0.4 ns, 1.5 ns, 6 ns, and a low intensity component at 140 ns consistent with back-scattered positrons forming Ps in vacuum), but no mesoporous lifetime components (in the range 10–120 ns) are observed. The sample foamed at 430 °C shows long-lived events that cannot be fitted with a single lifetime. At least two components (around 45 and 120 ns) are required in the POSFIT fitting, with the long lifetime component being indicative of diffusion and escape of Ps into the vacuum. This suspicion was confirmed by spectra acquired after the application of an 80 nm, sputter-deposited, Al capping layer that confines Ps to the porous film. The 120 ns component due to

^aElectronic mail: gidley@umich.edu

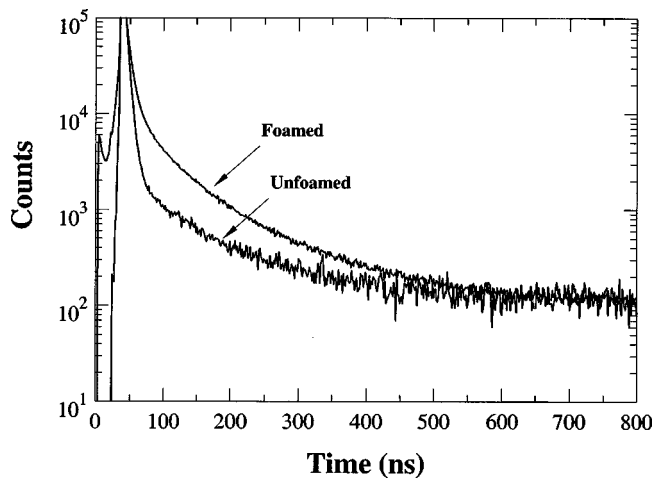


FIG. 1. The lifetime histograms comparing fully decomposed 10% PCL progen (foamed) with that of a similar sample prior to any decomposition (unfoamed). The formation of mesopores with long Ps lifetimes is evident.

escaping Ps disappeared as expected and lifetime components around 20 and 60 ns emerged, suggesting that only a fraction of the pores are interconnected. Thus, these films may have a complex, partially interconnected, pore structure. We will use the capped film spectra to eliminate specious results from the escape of Ps through the surface.

The lifetime histograms shown in Fig. 1 are given by dN_{Ps}/dt , where N_{Ps} is the total number of Ps annihilations recorded. (We fit only data having $t \geq 60$ ns, thus avoiding the bulk components whose lifetimes are all less than 6 ns.) We use the continuum fitting program, CONTIN,⁷ specialized for exponential lifetime analysis to obtain from these data a Ps lifetime distribution, $dN_{Ps}/d\tau$, where τ is the Ps lifetime (see Fig. 2). The uniqueness of this fitted distribution is a well-known issue with CONTIN.⁸⁻¹⁰ The peak widths in Fig. 2 are very sensitive to certain deconvolution parameters and should only be considered as typical of a class of statistically acceptable, bimodal lifetime distributions. The important result here is that both CONTIN and POSFIT find at least two, separable, lifetime components.

Given a statistically acceptable Ps lifetime distribution, $dN_{Ps}/d\tau$, the goal is to transform this distribution into a

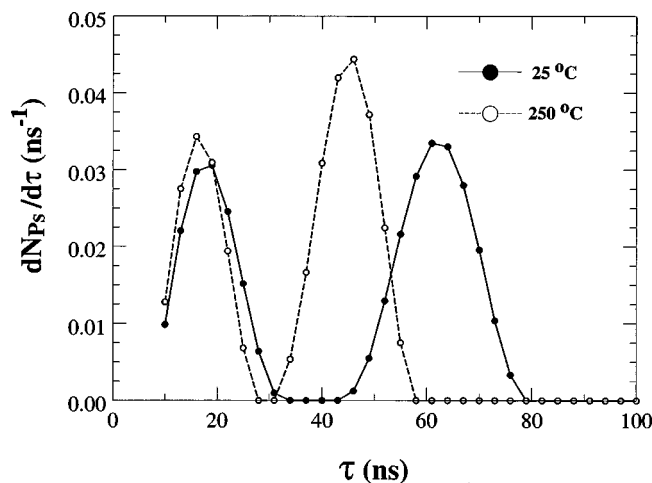


FIG. 2. The lifetime distributions fitted using CONTIN for an Al-capped sample of 10% PCL fully decomposed in MSSQ. The distribution is clearly shifted downward by the elevated sample temperature.

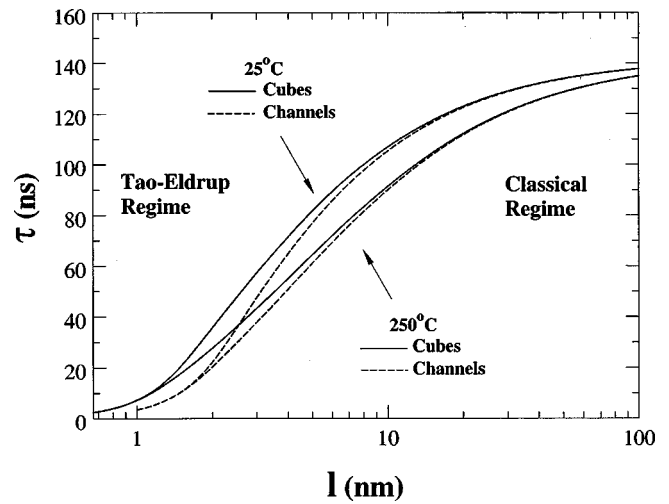


FIG. 3. The geometry and temperature dependence of the calculated Ps lifetime with mean free path in a pore. (See Ref. 2 for more details on the calculation.)

distribution of void sizes. More precisely, we can extract a relative distribution of specific void volume (void volume per unit sample volume) as a function of the void's mean-free path, l , which is given classically by $l = 4V_{\text{void}}/S_{\text{void}}$, where $V_{\text{void}}/S_{\text{void}}$ is the volume-to-surface area ratio in a particular void. We introduce l as a linear measure of pore size that in the large-pore limit does not depend on any assumed model of pore shape. To illustrate this point we have calculated² τ vs l for two different rectangular pore model geometries: three-dimensional (3D) cubes, and two-dimensional (2D) infinitely long square channels. As can be seen in Fig. 3 the curves are slightly model dependent in the quantum mechanical regime but merge for large pores.

We first consider the case of a specific but arbitrary void geometry for which the Ps lifetime in the void at a given temperature is a unique function of l . Given the function $\tau(l)$ for this geometry we can determine the size distribution of pores in which Ps annihilates,

$$\frac{dN_{Ps}}{dl} = \frac{dN_{Ps}}{d\tau} \frac{d\tau}{dl} \quad (1)$$

This distribution must be corrected for any pore size dependence in the trapping probability of Ps. Thus

$$\frac{dN_{Ps}}{dl} = \frac{dN_{\text{void}}}{dl} P_T, \quad (2)$$

where dN_{void}/dl is the void number-density distribution in l and P_T is the l -dependent specific trapping probability. If we write dV/dl as the specific void-volume distribution for the given void geometry, we have

$$\frac{dV}{dl} = \frac{dN_{\text{void}}}{dl} V_{\text{void}} = \frac{dN_{Ps}}{dl} \frac{V_{\text{void}}}{P_T} \quad (3)$$

Since Ps is formed in the solid material and must subsequently diffuse into the pores we expect Ps trapping to favor pores with large surface area. Thus, we assume $P_T \propto S_{\text{void}}$ and hence we find that $V_{\text{void}}/P_T \propto l$. The desired relation between specific void-volume distribution and Ps lifetime distribution for a particular void geometry is then given by

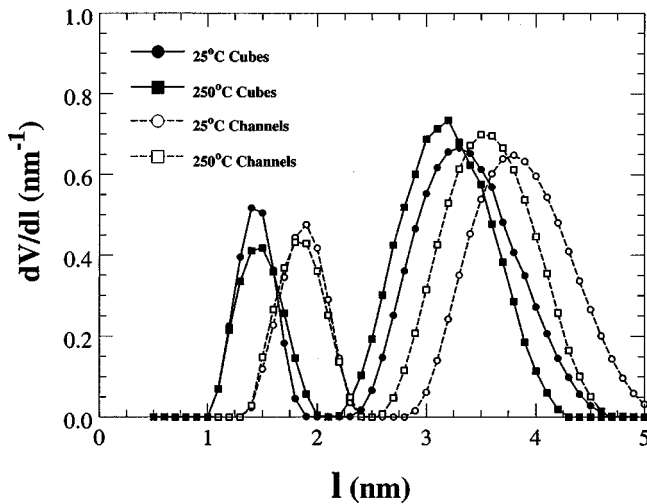


FIG. 4. The specific void-volume distributions derived from the transformation of the lifetime spectra in Fig. 2 using the corresponding lifetime calibration in Fig. 3. Each distribution is normalized to unity in total specific void-volume. The solid vs dashed curves represent the nominal dependence on the assumed shape of the pore.

$$\frac{dV}{dl} \propto \frac{dN_{Ps}}{d\tau} \frac{d\tau}{dl} l. \quad (4)$$

This particular distribution is especially convenient because it is rigorously pore-shape and pore model independent in the large-pore limit. Pore-shape dependence is only introduced through $\tau(l)$ (within the approximation that P_T depends on surface area but not explicitly on pore geometry).

Figure 4 shows the void volume distributions obtained from the lifetime distributions shown in Fig. 2 using the pore size calibrations presented in Fig. 3. The solid symbols and curves correspond to the high and low temperature results derived using a closed, cubic pore model of side length a [$l=(2/3)a$]. For comparison, the open symbols and dashed curves are the same spectra analyzed using an infinitely long, square-channel pore model ($l=a$). Although the lifetime distributions in Fig. 2 were acquired at two different temperatures and are therefore quite different, the deduced pore-size distributions in Fig. 4 are quite similar. This is an important systematic test of the model that demonstrates that Ps is thermally distributed throughout the entire void volume and not, for example, adsorbed on the void surface. The variation in the deduced specific void volume with the particular void-shape model (3D cubes vs 2D channels) probably represents a fundamental limitation of positronium physics. The systematically larger pore sizes deduced using the channels as compared with the cubic pores is indicative of a typical systematic error that should be assigned in the determination of these distributions.

In this particular MSSQ film a bimodal distribution of lifetimes is fitted by CONTIN (and POSFIT) which then transforms into a bimodal pore distribution. The relative intensities of the two peaks are not invariant under the transformation because of the linear factor of l in Eq. (4). The relative peak intensities of the lifetime distribution (40% and 60% for the short and long lifetime peaks, respectively) then become 24% and 76% in the relative void volume fraction. However, these relative intensities would have been much more skewed to roughly 5% and 95%, respectively, had we not

assumed that Ps trapping depended on the pore surface area. Hence, the reasonable assumption that $P_T \propto S_{\text{void}}$ is important to quantitative interpretation of the pore-size distribution and future PALS work should attempt to test this hypothesis. Nonetheless, we have presented a physical model that provides the basis for transforming a Ps lifetime distribution into a pore size distribution that becomes (as it should) completely pore-model independent in the limit of large pores.

Quantitative comparison with transmission electron microscopy (TEM) presented in Ref. 4 (using a similar 10% PCL in MSSQ sample) is complicated by the fact that TEM produces a 2D projection of a 100 nm slice of the film. Digital image analysis is found to be highly sensitive to the selected image contrast. However, simple visual analysis of the micrograph clearly distinguishes two size scales: there is an overall mottling of the image at a scale of about 4 nm and there are clearly what appear to be pores at the 10–20 nm level. The PALS data substantiate the 4 nm size scale but give no indication of pores with mean free paths larger than 5 nm. Assuming that these big pores observed by TEM are not artifacts of thin sample preparation then the PALS data suggest that these pores are irregular in shape (e.g., flattened or cellular) so as to produce $l \approx 3\text{--}4$ nm. While no definitive comparison can be made on the basis of this one film it appears from PALS that l in the pores is smaller than would naively be deduced from simple visual inspection of the TEM image. Unaccountably low Ps lifetimes could be consistent with enhanced annihilation at the pore surface due, for example, to Van der Waals attraction or activation of paramagnetic (spin flip) quenching centers.¹¹ These surface effects are not considered in the simple Tau–Eldrup model (which is explicitly material independent). Although the pore-size calibration appears to be quite accurate in silica,² further comparison of PALS results with TEM images, neutron scattering analysis, and gas absorption results is imperative for quantitative interpretation in other materials. For fully closed-pore films depth profiling³ with PALS can also search for depth-dependent inhomogeneities.

We thank Todd Ryan and Huei Min Ho at Sematech for helpful discussions. This research is supported by NSF Grant No. ECS-9732804 and by the Low- K Dielectric Program at Sematech.

¹W. L. Wu, W. E. Wallace, E. K. Lin, G. W. Lynn, C. J. Glinka, E. T. Ryan, and H.-M. Ho, *J. Appl. Phys.* **87**, 1193 (2000).

²D. W. Gidley, W. E. Frieze, A. F. Yee, T. L. Dull, E. T. Ryan, and H.-M. Ho, *Phys. Rev. B* **60**, R5157 (1999).

³M. P. Petkov, M. H. Weber, K. G. Lynn, K. P. Rodbell, and S. A. Cohen, *J. Appl. Phys.* **86**, 3104 (1999).

⁴C. V. Nguyen, K. R. Carter, C. J. Hawker, J. L. Hedrick, R. L. Jaffe, R. D. Miller, J. F. Remenar, H.-W. Rhee, P. M. Rice, M. F. Toney, M. Trollsas, and D. Y. Yoon, *Chem. Mater.* **11**, 3080 (1999).

⁵L. Xie, G. B. DeMaggio, W. E. Frieze, J. DeVries, D. W. Gidley, H. A. Hristov, and A. F. Yee, *Phys. Rev. Lett.* **74**, 4947 (1995).

⁶G. B. DeMaggio, W. E. Frieze, D. W. Gidley, M. Zhu, H. A. Hristov, and A. F. Yee, *Phys. Rev. Lett.* **78**, 1524 (1997).

⁷S. W. Provencher, *Comput. Phys. Commun.* **27**, 213 (1982).

⁸R. B. Gregory, *J. Appl. Phys.* **70**, 4665 (1991).

⁹S. Dannefaer, D. Kerr, D. Craigen, T. Bretagnon, T. Taliercio, and A. Foucaran, *J. Appl. Phys.* **79**, 9110 (1996).

¹⁰G. Dlubek, C. Hubner, and S. Eichler, *Nucl. Instrum. Methods Phys. Res. B* **142**, 191 (1998).

¹¹H. Saito and T. Hyodo, *Phys. Rev. B* **60**, 11070 (1999).